

Finite element analysis of lordosis restoration with anterior longitudinal ligament release and lateral hyperlordotic cage placement

Juan S. Uribe¹ · Jeffrey E. Harris² · J. M. Beckman¹ · Alexander W. L. Turner² · Gregory M. Mundis³ · Behrooz A. Akbarnia³

Received: 21 November 2014 / Revised: 27 February 2015 / Accepted: 8 March 2015 / Published online: 13 March 2015
© Springer-Verlag Berlin Heidelberg 2015

Abstract

Purpose Restoring sagittal alignment is an important factor in the treatment of spinal deformities. Recent investigations have determined that releasing the anterior longitudinal ligament (ALL) and placing hyperlordotic cages can increase lordosis, while minimizing need for 3 column osteotomies. The influences of parameters such as cage height and angle have not been determined. Finite element analysis was employed to assess the extent of lordosis achievable after placement of different sized lordotic cages.

Methods A 3-dimensional model of a L3–4 segment was used. Disc distraction was simulated by inserting interbody cages mid-body in the disc space. Analyses were performed in the following conditions: (1) intact, (2) ALL release, (3) ALL release + facetectomy, and (4) ALL release + posterior column osteotomy. Changes in segmental lordosis, disc height, foraminal height, and foraminal area were measured.

Results After ALL resection and insertion of hyperlordotic cages, lordosis was increased in all cases. The lordosis achieved by the shorter cages was less due to posterior disc height maintained by the facet joints. A facetectomy increased segmental lordosis, but led to contact between the spinous processes. For some configurations, a posterior column osteotomy was required if the end goal was to match cage angle to intradiscal angle.

Conclusion Increased segmental lumbar lordosis is achievable with hyperlordotic cages after ALL resection. Increased cage height tended to increase the amount of lordosis achieved, although in some cases additional posterior bone resection was required to maximize lordosis. Further studies are needed to evaluate the impact on regional lumbar lordosis.

Keywords Deformity correction · Finite element analysis · Anterior longitudinal ligament release · Sagittal alignment · Spine

Introduction

Restoration of sagittal alignment is one of the primary objectives in spinal deformity correction. The mainstay of treatment has been the traditional open approach in which a facetectomy, posterior column osteotomy (PCO), or pedicle subtraction osteotomy was performed [1–9]. Recent investigations have demonstrated that anterior column realignment (ACR) surgery which selectively releases the anterior longitudinal ligament (ALL), and annulus and placement of hyperlordotic cages through the minimally invasive lateral transpoas approach (MIS LIF) can increase lumbar lordosis while minimizing the need for 3-column osteotomies [10–16]. However, the optimal relationship between interbody cage design parameters, such as lordotic angle and posterior height, and resultant segmental lordosis require further investigation.

In this study, a three-dimensional, finite element model of a L3–4 lumbar segment, including ligamentous components, was developed to investigate the changes in segmental lordosis, anterior disc height (ADH), and posterior disc height (PDH) achieved with ALL release and insertion

✉ Juan S. Uribe
juribe@health.usf.edu

¹ University of South Florida, 2 Tampa General Circle, 7th Floor, Tampa, FL 33606, USA

² NuVasive, Inc, San Diego, CA, USA

³ San Diego Center for Spinal Disorders, La Jolla, CA, USA

of different posterior height and lordosis angled cages from the lateral position. The constraints to segmental lordosis and disc height provided by the osseous anatomy were also investigated by simulating posterior osteotomies; namely a facetectomy and PCO.

Materials and methods

Finite element model

A 3-dimensional, finite element model of a L3–4 ligamentous spine segment was created using CT data from a moderately degenerated 55-year-old male cadaveric spine (Fig. 1a). The spine geometry was obtained from CT data using manual and automatic segmentation techniques (Scan IP Version 6.0, Simpleware, Exeter, UK). The spinal ligaments were represented using tension-only nonlinear springs (ANSYS 15.0, Canonsburg, PA, USA) [17, 18]. The major spinal ligaments used in the model were anterior longitudinal ligament (ALL), posterior longitudinal ligament (PLL), ligamentum flavum (LF), interspinous ligament (ISL), supraspinous ligament (SSL), and the capsular ligament (CL). The insertion points of the ligaments were approximated to match typical anatomy. Nonlinear constitutive material properties were applied to each ligament.

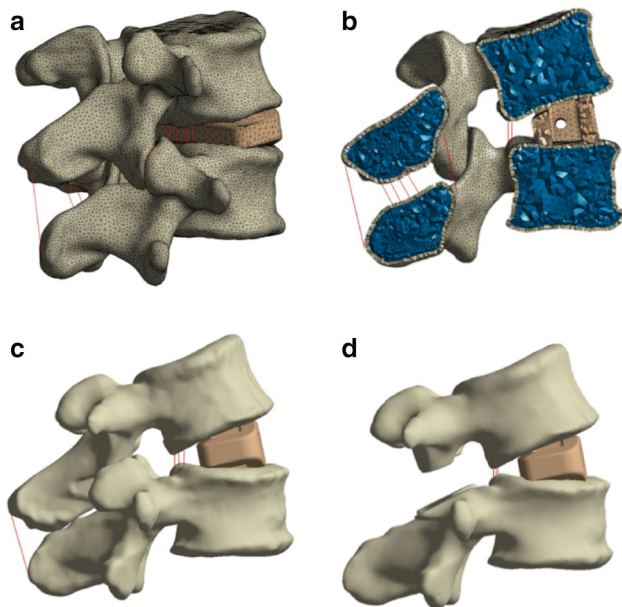


Fig. 1 Predicted displacement of the L3–4 spine segment after insertion of an 8 mm posterior height \times 20° lordosis cage and anterior longitudinal ligament release. **a** The L3–4 ligamentous finite element model was created from a 55-year-old male cadaveric spine. **b** Sagittal cross-section view of the model with intact posterior elements. **c** Lateral view after facetectomies. Note spinous process impingement. **d** Lateral view after a posterior column osteotomy

The material properties of each structure in the model are shown in Table 1. The residual intervertebral disc was not included in the model since it was assumed that the residual disc properties would have minimal impact on segmental lordosis.

Boundary conditions

The inferior endplate of L4 was rigidly fixed and the L3–4 level was “virtually” implanted with lordotic interbody cages that were positioned midway between the anterior and posterior margins of the disc space. Distraction of the disc space was simulated by allowing L3 to translate and rotate until the contact interface between the vertebral endplates and the interbody cage achieved static equilibrium. This resulted in distraction and sagittal realignment of L3. The contact between the facet joints was simulated as frictionless surfaces. Simulations were performed using ANSYS with the following conditions: (1) a baseline comparator model consisting of an interbody cage with 9 mm posterior height \times 10° lordosis and the ALL intact, (2) ALL release with intact posterior elements (IPE), (3) ALL release combined with a facetectomy, and (4) ALL release combined with a PCO (Fig. 1b–d). Conditions 2, 3, and 4 were each tested with 6, 8, and 10 mm cages with angles of 20° and 30°. With these conditions a total of 19 different models were simulated and compared (Table 2). The results from these models were also compared to the “pre-operative” spinal segment measurements.

Data analysis

The results measured in each model included segmental lordosis, intradiscal angle, foraminal height, sagittal foraminal area, anterior disc height (ADH), and posterior disc height (PDH). Segmental lordosis was defined as the angle between the inferior endplate of L4 and the superior endplate of L3. The intradiscal angle was defined as the angle between the superior endplate of L4 and the inferior endplate of L3. Foraminal height was defined as the cranio-caudal distance between the pedicles, measured in the sagittal plane. Sagittal foraminal area was approximated by an ellipse defined by the foraminal height (“*a*”) and the anteroposterior width (“*b*”), measured perpendicular to *a*. The anteroposterior width was defined as the length

Table 1 Summary of material properties

Property	<i>E</i> (MPa)	ν	References
Cortical bone	12,000	0.2	Goel [16], Polikeit [17]
Cancellous bone	300	0.2	Morgan [18]
Ligaments	Hyperelastic	N/A	Schmidt [15]

Table 2 Summary of models created and condition tested

Condition	ALL	Posterior elements	Cage posterior height (mm)	Cage lordotic angle (deg)
1	Intact	Intact	9	10
2	Released	Intact	6	20
			8	
			10	
			6	30
			8	
			10	
3	Released	Facetectomy	6	20
			8	
			10	
			6	30
			8	
			10	
4	Released	PCO	6	20
			8	
			10	
			6	30
			8	
			10	

PCO posterior column osteotomy

between the inferoposterior corner of the L3 vertebral body and the articular process of the facet joint. The area was calculated using the ellipse formula $\pi ab/2$, where a and b are the major and minor axes of the ellipse [19]. ADH was defined as the minimum distance between the anterior margins of the disc space. PDH was defined as the minimum distance between the posterior margins of the disc space.

Results

Segmental lordosis

The baseline model (9 mm × 10° cage) with an intact ALL had a segmental lordosis of 14°. Resection of the ALL and placement of 20° and 30° hyperlordotic cages gave more segmental lordosis than placement of the 10° cage without ALL resection. With IPE, ALL resection, and insertion of the hyperlordotic 20° and 30° cages, lordosis increased by 1°–10° (7–71 % increase from baseline) in all cases. The facet joints prevented the shorter 20° cages from achieving greater lordosis by maintaining PDH (Fig. 2a).

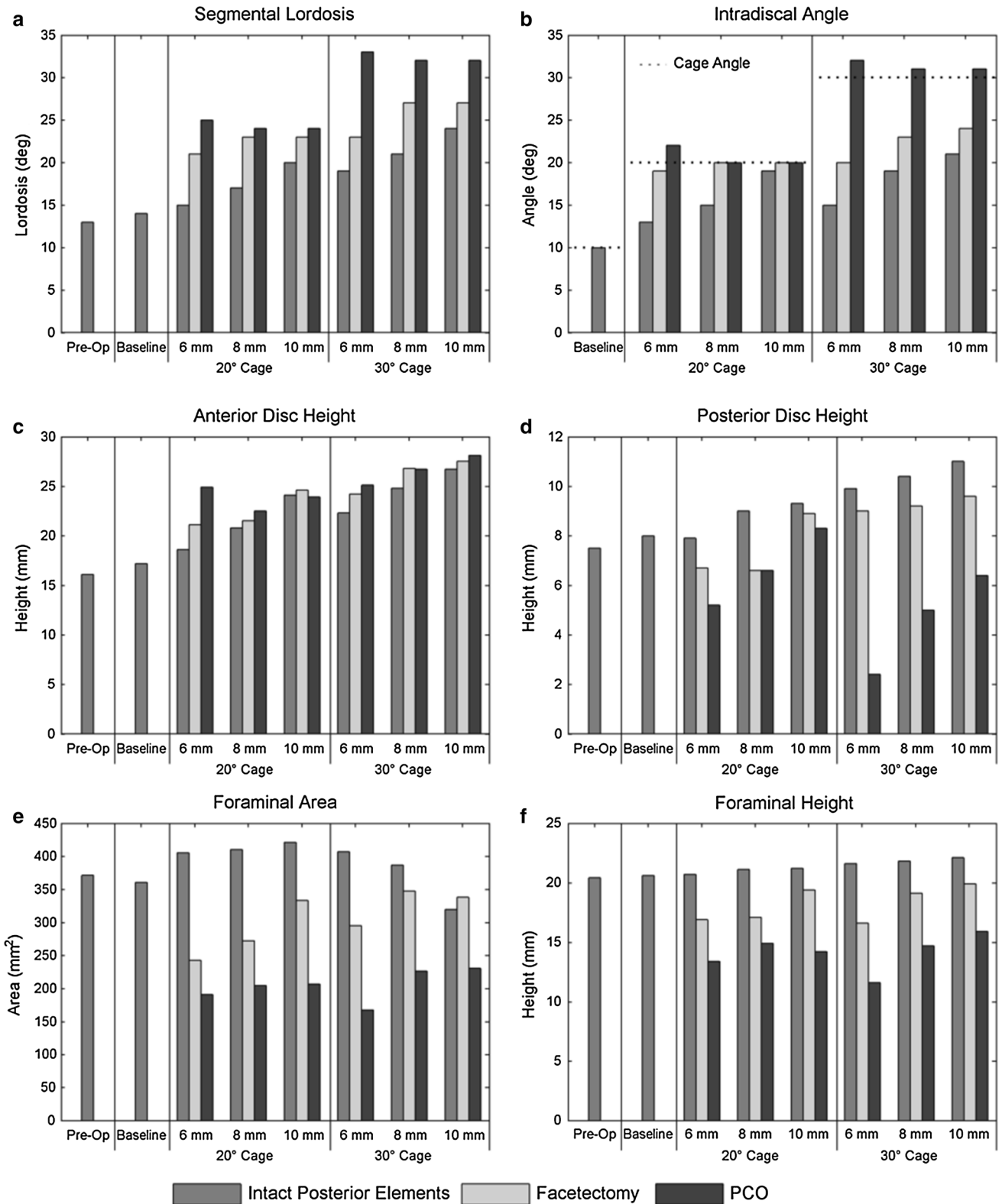
A facetectomy increased segmental lordosis for both the 20° and 30° cages. All spine segments in this test group achieved segmental lordosis ranging from 21° to 27°. Further increases in lordosis with the facetectomy condition were restricted by impingement of the spinous

Fig. 2 Results of finite element simulation of anterior longitudinal ligament release and insertion of 20° and 30° lordotic cages of 6, 8, and 10 mm posterior heights with intact posterior elements, facetectomies, or posterior column osteotomies. **a** Segmental lordosis compared to the pre-operative (intact segment) and baseline construct (9 mm posterior height × 10° lordosis cage with intact anterior longitudinal ligament). **b** Intradiscal angle compared to the baseline construct. *Dashed lines* indicate the implanted cage lordosis angles. **c** Anterior disc height compared to the pre-operative and baseline conditions. **d** Posterior disc height compared to the pre-operative and baseline conditions. **e** Sagittal foraminal area compared to the pre-operative (intact) and baseline conditions. **f** Foraminal height compared to the pre-operative and baseline conditions

processes (Fig. 1c). APCO was required for the 30° cages if the goal was to match the cage lordosis. In these cases, 32°–33° lordosis was achieved.

Intradiscal angle

With IPE, intradiscal angles were between 13°–19° for the 20° cages, and 15°–21° for the 30° cages. Only the 10 mm × 20° cage resulted in an intradiscal angle that closely matched the cage angle (Fig. 2b). A facetectomy allowed for an increase in intradiscal angle with the 20° cages having an intradiscal angle of 19°–20° and the 30° cages having an intradiscal angle of 20°–24°. Each of the 20° cages with a facetectomy had an intradiscal angle that closely matched cage angle. For the 30° cages, increases in



intradiscal angle were restricted by impingement of the spinous processes. The PCO condition resulted in close conformity between the cage angle and intradiscal angle, with intradiscal angles measuring between 30° and 33° for all cages.

Disc heights

For the 20° cages with IPE, the change in PDH from baseline ranged from 99 to 116 % and ADH from 108 to 138 %. The 30° cages change in PDH ranged from 124 to 138 % and ADH 130 to 155 % with respect to baseline (Fig. 2c, d). A facetectomy with 20° cages resulted in PDHs decreasing to 83–84 % from baseline for the 6 and 8 mm cages, and increasing to 111 % for the 10 mm cage. The 30° cages had PDHs ranging from 113 to 120 % from baseline. ADH increased to 123–151 % for the 20° cages, and 141–160 % for the 30° cages. With a PCO the PDH decreased in all cases, to as low as 30 % of baseline with the 6 mm posterior height cage. ADH increased to 138–145 % for the 20° cages, and to 146–163 % for the 30° cages. For a given cage configuration (angle and height), ADH changed by 23–63 % after the facetectomy and PCO, while PDH changed by 4–70 %.

Foraminal height

With IPE, the foraminal height increased 0.4–7 % for all conditions compared to baseline. A facetectomy and PCO resulted in decreased height (Fig. 2e). The foraminal height increased as cage height increased. With a facetectomy, the 10 mm × 20° and 30° cages approached the original baseline height (foraminal height was within 3–6 % of height of baseline). A PCO resulted in the largest reductions of foraminal height, with the height decreasing 23–44 % from baseline.

Foraminal area

With the 20° cages and IPE, foraminal area increased 12–15 % with respect to baseline. With the 30° cages, foraminal area decreased as cage height increased. The 6 mm × 30° and 8 mm × 30° cages had area increases of 13 and 7 %, respectively, while the 10 mm × 30° decreased by 11 % (Fig. 2f). A facetectomy reduced the foraminal area compared to the baseline in all cases. An increase in cage height corresponded to an increase in foraminal area, although the area was still less than the baseline. The 20° cages decreased the area by 8–33 %, while the 30° cages decreased the area by 6–18 %. A PCO further reduced the foraminal area, with the decrease in area ranging from 36 to 54 % with respect to baseline.

Discussion

Sagittal imbalance has been shown to be a primary source of symptomatology among adult spinal deformity cases. Patients suffering from this pathology typically demonstrate that a loss of lumbar lordosis creating a positive sagittal balance as the spinopelvic harmony is disrupted. This, in turn, causes undue stress and exhaustion of the lumbar postural muscles and results in generalized back pain [12, 20–22]. Therefore, one of the primary objectives in ASD is restoration of lumbar lordosis thereby correcting sagittal balance. This is commonly accomplished with posterior based osteotomies, ranging from multilevel PCO's to 3-column osteotomies. The PCO involves resection of bilateral facets, interspinous ligament, and ligamentum flavum at the selected level which can yield up to 10° of lordosis per osteotomy [2, 4, 5]. This is a relatively safe technique and can be performed at multiple levels. The pedicle subtraction osteotomy (PSO), conversely, is a technically challenging procedure and is associated with significant blood loss and morbidity; however, it can yield 25°–40° of lordosis at a single level depending on the technique [1, 3, 4, 7, 23, 24].

An alternative method is an ACR procedure that involves selective sectioning of the ALL and anterior annulus and placement of hyperlordotic cages through the lateral transpsoas approach. This technique has been shown to increase lumbar lordosis, while minimizing the need for 3-column osteotomies [10–13, 25]. Furthermore, it has been shown to be equivalent to a PSO in achieving segmental lordosis [12–14]. In order to optimize lordosis gained through this approach, we studied different cage angulations and heights as well as the incorporation of posterior osteotomies to the construct.

The specimen used in this model had a “pre-operative” segmental lordosis of 13°. In this analysis, we demonstrated that, combined with an ALL section, the 10 mm × 20° hyperlordotic cage achieved a segmental lordosis of 20° and the 10 mm × 30° hyperlordotic cage achieved a segmental lordosis of 24° without interruption of the posterior elements, representing a 7° and 11° increase with respect to the “pre-operative” condition, respectively. This is consistent with previously published results and places the findings in the model close to what was observed in both clinical and cadaveric studies where hyperlordotic cages were implanted without posterior releases [12, 13]. In a cadaveric radiographic study, Uribe et al. [13] reported an average increase in lordosis from pre-operative of $9.5 \pm 3.3^\circ$ with 20° cages and $11.6 \pm 3.6^\circ$ with 30° cages. In that study, average posterior cage heights were shorter than the simulation performed here, closer to 6 mm, potentially due to more degenerated

cadaveric specimens. Manwaring et al. reported lordosis improvement of 12° per anterior column release (ACR) level using a 30° hyperlordotic cage with an 8 mm posterior height (1 year follow-up) [12, 13].

In addition to restoring lordosis, it is important to maximize the surface area contact between the entire surface of the interbody cage and the vertebral endplate. Poor mismatch between the cage and endplate can result in high stresses at the bone–implant interface and possibly lead to subsidence when the posterior elements are not released and lead to inadequate end plate coverage from too much lordosis when the posterior element are released. The intradiscal angle was measured as a way of quantifying whether the cage had good contact with the endplate. With IPE only the 10 mm × 20° cage resulted in an intradiscal angle that closely matched the cage angle. The other configurations resulted in only the anterior region of the cage coming in contact with the endplate. When a facetectomy was utilized, the intradiscal angle for the 20° cages ranged between 19° and 20°, indicating close contact along the bone–implant interface. For the 30° cages, a PCO was required to ensure a close match between cage angle and intradiscal angle.

In both the intact posterior elements and facetectomy groups, an increase in posterior cage height generally correlated with an increase in segmental lordosis in both the 20° and 30° groups. In the facetectomy group, the lordosis achieved was limited by spinous process impingement. Interestingly, we found that the 20° cage with both the 8 and 10 mm posterior height was slightly superior in achieving segmental lordosis than the 30° cage with only a 6 mm posterior height. The 30° cage with larger posterior heights then outperformed the above two. The reasoning for this is the 30° cages did not allow for more angulation due to posterior height being maintained by spinous process impingement. The 30° cages also had poor mismatch between the cage angle and intradiscal angle without PCO.

The 10 mm × 30° cage with IPE achieved the largest amount of segmental lordosis, with increases in lordosis equivalent to the standard PCO in terms of radiographic outcomes [12]. However, it should be noted that in this configuration, only the anterior margin of the cage maintained contact with the vertebral endplate. If lordosis equivalent to a pedicle subtraction osteotomy is desired, then an ACR combined with a 30° hyperlordotic cage would be the ideal configuration as this was shown to achieve 32° lordosis. Further in vitro (cadaveric or computational) and clinical studies would need to validate this.

Despite the large change of lordosis seen in all groups, smaller changes in anterior disc height were noted, including those with posterior releases (Fig. 1c). This is especially evident with the lordosis achieved by 30° cages

in the PCO group. This finding suggests that most lordosis is achieved through changes of posterior disc height in relation to a relative stable anterior disc height. For example, in this model, the shortest 20° and 30° cages combined with a PCO resulted in the most lordosis while changes in anterior disc height generally remained comparable to the IPE and facetectomy conditions. A potential benefit of minimizing changes in anterior disc height is avoiding direct vessel injury and avulsion. Mobilization of intraluminal plaques and prevention of embolic events would also be minimized.

When considering cage selection/design, it is important to understand the goal of surgery. If the goal is to achieve the most segmental lordosis without disruption of the posterior elements, then the ideal combination, in this model, would be sectioning the ALL combined with a 10 mm × 20° cage. As mentioned previously, this cage provided the most lordosis while maintaining contact along the bone–interbody interface, the foraminal height, and sagittal area. The ideal cage size and angle while maintaining IPE will vary between patients.

If a posterior resection is required to allow for more lordosis, caution should be taken to avoid impingement of the exiting nerve roots. In this model, the 6 mm × 30° cage with a PCO produced the largest changes in foraminal dimensions. There was a 70 % decrease in PDH, while the foraminal height was decreased by only 44 %. The foraminal area was reduced by 53 % which could result in nerve root compression. When selecting and trialling cage sizes, care should also be taken to ensure there is good contact between the interbody cage and the vertebral endplate, noting that over-distraction may also place high stress on the endplates.

Limitations

While initial results from this study are promising, further investigation is needed to evaluate how changes in segmental lordosis after ACR impact regional lumbar lordosis and sagittal alignment. It must be emphasized that this work only focused on the effects on segmental lordosis at a single level and does not address any potential global compensatory mechanisms of the spine after cage placement. In reality a large number of muscles are involved in maintaining the stability of the spine. In our model, the external muscle forces were ignored and assumed to have small impact on the amount of lordosis achieved from implantation of the hyperlordotic cages. Furthermore it was assumed the residual intervertebral disc would have negligible effect on the amount of lordosis achieved, and therefore the disc was ignored in the model. This study also did not address any potential posterior fixation and compression techniques, which may lead to increased lordosis.

Finally, additional work is needed to determine the effects of cage placement within the disc space, and whether there is an ideal anterior-posterior position for the cage.

Conclusion

Anterior column realignment and insertion of increasingly lordotic cages led to a mean progressive increase in segmental lordosis. The addition of posterior osteotomies reduced posterior disc heights while further increasing lordosis, with the spinous processes inhibiting angulation in the facetectomy group. The change in anterior disc height was relatively small between the different configurations, suggesting that a change in lordosis is primarily governed by the posterior disc height. The addition of posterior releases led to greater increases in lordosis. However, the addition of a posterior release did not always result in uniform contact between the interbody cage and the vertebral endplate. The 30° cages required a PCO if it was desired to maintain uniform contact between the cage and endplate. The optimal combination of cage design and surgical intervention will be better understood through clinical application.

Conflict of interest Dr. Uribe is a consultant for NuVasive, Inc., from which he has also received clinical/research support for the study. Dr. Akbarnia owns stock in NuVasive, Inc., and is a consultant for the company. Dr. Mundis is a consultant and receives royalties for NuVasive, Inc. Dr. Turner and Mr. Harris are employees of NuVasive, Inc., and own stock in the company.

References

- Bridwell KH, Lewis SJ, Lenke LG, Baldus C, Blanke K (2003) Pedicle subtraction osteotomy for the treatment of fixed sagittal imbalance. *J Bone Joint Surg Am* 85-A:454–463
- Bridwell KH (2006) Decision making regarding Smith-Petersen vs. pedicle subtraction osteotomy vs. vertebral column resection for spinal deformity. *Spine* 31:S171–S178
- Buchowski JM, Bridwell KH, Lenke LG et al (2007) Neurologic complications of lumbar pedicle subtraction osteotomy: a 10-year assessment. *Spine* 32:2245–2252
- Cho KJ, Bridwell KH, Lenke LG, Berra A, Baldus C (2005) Comparison of Smith-Petersen versus pedicle subtraction osteotomy for the correction of fixed sagittal imbalance. *Spine* 30:2030–2037
- Gill JB, Levin A, Burd T, Longley M (2008) Corrective osteotomies in spine surgery. *J Bone Joint Surg Am* 90:2509–2520
- Godde S, Fritsch E, Dienst M, Kohn D (2003) Influence of cage geometry on sagittal alignment in instrumented posterior lumbar interbody fusion. *Spine* 28:1693–1699
- Lafage V, Schwab F, Vira S et al (2011) Does vertebral level of pedicle subtraction osteotomy correlate with degree of spinopelvic parameter correction? *J Neurosurg Spine* 14:184–191
- Schwab FJ, Patel A, Shaffrey CI et al (2012) Sagittal realignment failures following pedicle subtraction osteotomy surgery: are we doing enough? Clinical article. *J Neurosurg Spine* 16:539–546
- Berjano P, Aebi M (2015) Pedicle subtraction osteotomies (PSO) in the lumbar spine for sagittal deformities. *Eur Spine J* 24(Suppl 1):49–57
- Deukmedjian AR, Dakwar E, Ahmadian A, Smith DA, Uribe JS (2012) Early outcomes of minimally invasive anterior longitudinal ligament release for correction of sagittal imbalance in patients with adult spinal deformity. *Sci World J* 2012:789698
- Deukmedjian AR, Le TV, Baaj AA, Dakwar E, Smith DA, Uribe JS (2012) Anterior longitudinal ligament release using the minimally invasive lateral retroperitoneal transpoas approach: a cadaveric feasibility study and report of 4 clinical cases. *J Neurosurg Spine* 17:530–539
- Manwaring JC, Bach K, Ahmadian AA, Deukmedjian AR, Smith DA, Uribe JS (2014) Management of sagittal balance in adult spinal deformity with minimally invasive anterolateral lumbar interbody fusion: a preliminary radiographic study. *J Neurosurg Spine* 20:515–522
- Uribe JS, Smith DA, Dakwar E et al (2012) Lordosis restoration after anterior longitudinal ligament release and placement of lateral hyperlordotic interbody cages during the minimally invasive lateral transpoas approach: a radiographic study in cadavers. *J Neurosurg Spine* 17:476–485
- Akbarnia BA, Mundis GM Jr, Moazzaz P et al (2014) Anterior column realignment (ACR) for focal kyphotic spinal deformity using a lateral transpoas approach and ALL release. *J Spinal Disord Tech* 27:29–39
- Berjano P, Damilano M, Lamartina C (2012) Sagittal alignment correction and reconstruction of lumbar post-traumatic kyphosis via MIS lateral approach. *Eur Spine J* 21:2718–2720
- Berjano P, Lamartina C (2013) Far lateral approaches (XLIF) in adult scoliosis. *Eur Spine J* 22(Suppl 2):S242–S253
- Rohlmann A, Bauer L, Zander T, Bergmann G, Wilke HJ (2006) Determination of trunk muscle forces for flexion and extension by using a validated finite element model of the lumbar spine and measured in vivo data. *J Biomech* 39:981–989
- Schmidt H, Heuer F, Drumm J, Klezl Z, Claes L, Wilke HJ (2007) Application of a calibration method provides more realistic results for a finite element model of a lumbar spinal segment. *Clin Biomech* 22:377–384
- Hegazy RM, Abdelrahman AY, Azab WA (2014) Computed tomographic evaluation of C5 root exit foramen in patients with cervical spondylotic myelopathy. *Surg Neurol Int* 5:S59–S61
- Grubb SA, Lipscomb HJ (1992) Diagnostic findings in painful adult scoliosis. *Spine (Phila Pa 1976)* 17:518–527
- Isaacs RE, Hyde J, Goodrich JA, Rodgers WB, Phillips FM (2010) A prospective, nonrandomized, multicenter evaluation of extreme lateral interbody fusion for the treatment of adult degenerative scoliosis: perioperative outcomes and complications. *Spine* 35:S322–S330
- Schwab F, Lafage V, Patel A, Farcy JP (2009) Sagittal plane considerations and the pelvis in the adult patient. *Spine (Phila Pa 1976)* 34:1828–1833
- Baldus CR, Bridwell KH, Lenke LG, Okubadejo GO (2010) Can we safely reduce blood loss during lumbar pedicle subtraction osteotomy procedures using tranexamic acid or aprotinin? A comparative study with controls. *Spine (Phila Pa 1976)* 35:235–239
- Mummaneni PV, Dhall SS, Ondra SL, Mummaneni VP, Berven S (2008) Pedicle subtraction osteotomy. *Neurosurgery* 63:171–176
- Costanzo G, Zoccali C, Maykowski P, Walter CM, Skoch J, Baaj AA (2014) The role of minimally invasive lateral lumbar interbody fusion in sagittal balance correction and spinal deformity. *Eur Spine J* 23(Suppl 6):699–704